

Accepted Manuscript

Title: High performance stoichiometric Cu₂S cathode on carbon fiber current collector for lithium batteries

Author: Gulnur Kalimuldina Izumi Taniguchi

PII: S0013-4686(16)32604-4

DOI: <http://dx.doi.org/doi:10.1016/j.electacta.2016.12.058>

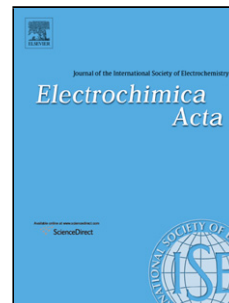
Reference: EA 28530

To appear in: *Electrochimica Acta*

Received date: 14-10-2016

Revised date: 7-12-2016

Accepted date: 9-12-2016



Please cite this article as: Gulnur Kalimuldina, Izumi Taniguchi, High performance stoichiometric Cu₂S cathode on carbon fiber current collector for lithium batteries, *Electrochimica Acta* <http://dx.doi.org/10.1016/j.electacta.2016.12.058>

This is a PDF file of an unedited manuscript that has been accepted for publication. As a service to our customers we are providing this early version of the manuscript. The manuscript will undergo copyediting, typesetting, and review of the resulting proof before it is published in its final form. Please note that during the production process errors may be discovered which could affect the content, and all legal disclaimers that apply to the journal pertain.

High performance stoichiometric Cu₂S cathode on carbon fiber current collector for lithium batteries

Gulnur Kalimuldina^a, Izumi Taniguchi^{b,*}

^aDepartment of Chemical Engineering, Tokyo Institute of Technology, Tokyo 152-8552, Japan

^bDepartment of Chemical Science and Engineering, Tokyo Institute of Technology, Tokyo 152-8552, Japan

Abstract

In this study, stoichiometric Cu₂S with monoclinic crystal structure with space group $P2_1/c$ was prepared *via* spray pyrolysis with followed heat treatment. Its electrochemical properties were investigated after coating on a carbon fiber paper (CFP) current collector and cycling at various cut-off voltages. The reversible stable capacity of about 330 mAh g⁻¹ (98 % of its theoretical capacity) exhibited by the cell for 20 cycles at 0.1 C and slightly dropped to 311 mAh g⁻¹ after 50 cycles. At higher 1 C rate, a discharge capacity of 280 mAh g⁻¹ was retained for 100 cycles with approximately 100 % Coulombic efficiency between 1.0-3.0 V. While the gradual capacity decrease is observed with the increase of the discharge cut-off voltage to avoid solid electrolyte interface (SEI) formation during the 1st discharge. The cells showed capacities of 307 and 280 mAh g⁻¹ after the 5th cycle at 0.1 C when cycled between 1.1-3.0 V and 1.2-3.0 V, respectively, due to the lowered lithium ion diffusion. *Ex situ* XRD analysis of the recovered electrodes after cycling with near theoretical capacity allowed discussing the actual reaction mechanism of stoichiometric Cu₂S with Li⁺.

Keywords: copper sulfide, carbon fiber paper, lithium-ion battery, cathode, spray pyrolysis

*Corresponding author.

Tel. & Fax: +81-3-5734-2155

E-mail: taniguchi.i.aa@m.titech.ac.jp

1. Introduction

The increased demand for the sustainable energy is driving an enormous impact on the development of advanced storage systems by exploring new types of battery chemistries and configurations [1]. Traditional cathode materials based on the lithiated transition-metal oxide and phosphate are unable to satisfy the need for the combination of high energy density, safety and reduced cost required for EVs and smart grid [2,3]. As an alternative cathode material Cu_2S is gaining an interest due to its high capacity of 337 mAh g^{-1} and energy density of 553 Wh kg^{-1} . However, it has the hindrance of partial lithium polysulfide dissolution in organic electrolyte during cycling, which causes rapid capacity decay, loss of active material and poor cycle life [4,5]. So far, several Cu_2S preparation methods have been reported [6-10] and a few researchers [4,6] highlighted the effect of Al and Cu foil current collectors on the electrochemical performance of copper sulfides. In our previous work, the details of the failure mechanism of stoichiometric Cu_2S coated on an Al foil current collector due to the corrosion during cycling and its improvement on Cu foil were reported [11]. However, up to now the electrochemical properties of stoichiometric Cu_2S coated on carbon fiber paper (CFP) have not been investigated. In this work, CFP used as a current collector to increase the electron flow and Li^+ ion diffusion, to facilitate active electrode mass utilization and create a preferable condition for the investigation of the actual Cu_2S reaction mechanism with lithium. Moreover, carbon fiber will avoid corrosion problems tend to occur on Al and Cu current collectors.

Carbon materials are well known for their applicability for the improvement of electronic conductivity of cathode materials [12-14]. Carbon fiber is well-connected,

and its conductive structure and appropriate pore channels create an effective electron path as well as an effective condition for the electrolyte to access the active material [15]. Here we report simple preparation method of stoichiometric Cu_2S with monoclinic crystal structure by spray pyrolysis (SP) with followed heat treatment and that stable high capacity with a long cycle life can be achieved using CFP as a current collector without an involvement of the complex synthesis or the surface modifications.

Copper sulfide has varying stoichiometries, which significantly affect its structural and electrochemical properties [6,11]. Thus, we verified chemical composition of monoclinic Cu_2S by X-ray diffraction (XRD) and inductively coupled plasma-optical emission spectroscopy (ICP-OES) analyses before electrochemical testing. In addition, this study will provide insight into the fully charged/discharged stoichiometric Cu_2S electrode's behavior coated on CFP by *ex situ* XRD analysis after cycling at various cut-off voltage windows (1.0, 1.1, 1.2 to 3.0 V).

2. Experimental

2.1. Preparation of stoichiometric Cu_2S

Stoichiometric Cu_2S was prepared using SP method with further heat treatment. The precursor solution was prepared from copper nitrate trihydrate ($\text{Cu}(\text{NO}_3)_2 \cdot 3\text{H}_2\text{O}$) and thiourea ($\text{CS}(\text{NH}_2)_2$) dissolved in distilled water in the molar ratio of 1:1 at 0.05 M. All chemicals were purchased from Wako Pure Chemical Industries Ltd. The schematic diagram of the SP facility is described elsewhere [16]. The atomized precursor solution at a frequency of 1.7 MHz by ultrasonic nebulizer was carried

inside the vertical reactor by $N_2 + 3\% H_2$ gas atmosphere. The flow rate of the gas was fixed at $2 L min^{-1}$ and reactor temperature was $400\text{ }^\circ C$. The as-prepared sample was heat treated at the temperature of $460\text{ }^\circ C$ in $N_2 + 3\% H_2$ atmosphere for 2 h to obtain stoichiometric Cu_2S [11].

2.2. Material characterization

The crystalline phase of stoichiometric Cu_2S was characterized by powder X-ray diffraction (Ultima IV with D/tex Ultra, Rigaku) with $Cu-K\alpha$ radiation. The lattice parameters were determined by Rietveld refinement of the XRD data using PDXL (Rigaku, Ver. 1.8.1.0) software. To verify Cu/S molar ratio in the Cu_2S ICP-OES (Shimadzu, ICPS-7510) was used and the morphology of as-prepared Cu_2S was examined by field-emission scanning electron microscopy (FE-SEM, Hitachi, S4500).

2.3. Cell assembly and electrochemical measurements

Electrochemical measurements were performed with coin-type CR2032 cells with stoichiometric Cu_2S cathodes and lithium-metal foils. 1 M lithium bis(trifluoromethane sulfonamide) (LiTFSI) in 1,3-dioxolane (DOL) and dimethoxyethane (DME) with a volume ratio of 1:1 (Tomiya Pure Chemical Co., Ltd.) was used as an electrolyte. The electrode consisting of 80:10:10 wt. % of Cu_2S , acetylene black (AB) and polyvinylidene fluoride (PVDF) was dispersed in 1-methyl-2-pyrrolidinone (NMP). Then the as-made slurry was coated onto CFP (Toray Paper TGP-H-030 5% Wet Proofing) by using doctor blade technique and

dried at 60 °C for 4 h in a vacuum oven. Finally, circular disks were punched, and the mass loadings of Cu₂S were 1.5-2.0 mg per scrapped electrode square (100 mm²). All cells were fabricated inside an Ar filled glove box (99.9995 % purity).

The cells were galvanostatically cycled at the range of 1.0-3.0 V, 1.1-3.0 V, and 1.2-3.0 V versus Li/Li⁺ at 0.1 to 5 C on multichannel battery testers (Hokuto Denko, HJ1010mSM8A), respectively. The C-rates were based on the theoretical capacity of Cu₂S (337 mAh g⁻¹).

Cyclic voltammetry (CV) measurements were performed in the potential windows of 1.0, 1.1, 1.2 and 3.0 V (vs. Li/Li⁺) at a scanning rate of 0.05 mV s⁻¹. Electrochemical impedance spectroscopy (EIS) was carried out using a Solartron 1255B frequency response analyzer connected to a Solartron SI 1287 electrochemical interface. The amplitude of the ac signal was 10 mV in the frequency range from 100 kHz to 0.1 Hz. The electrochemical measurements were performed at room temperature.

For the *ex situ* XRD studies, the recovered electrodes after cycling were washed with DOL, dried inside an Ar gas atmosphere glove box at 60 °C for 2 h and protected from the air atmosphere by a Kapton[®] foil.

3. Results and discussion

The XRD pattern of prepared stoichiometric Cu₂S is shown in **Fig. 1**. The obtained XRD peaks are fitting with ICDD database pattern (00-033-0490) for the monoclinic Cu₂S crystal structure with space group *P2₁/c*. No peaks arising from impurities can be detected. The lattice constants of a= 15.237 Å, b= 11.884 Å, and c= 13.492 Å obtained by Rietveld refinement are matching with the values reported in

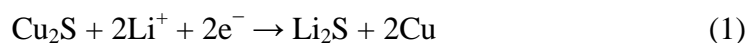
the literature [17]. This sample was analyzed by ICP-OES, and it revealed that the Cu/S molar ratio equals to two, which confirms stoichiometric ratio. The morphology of spherical particles less than 1 μm in size demonstrated in FE-SEM image within Fig. 1.

Electrochemical properties of stoichiometric Cu_2S coated on a CFP current collector at cut-off voltage window of 1.0-3.0 V were investigated by galvanostatic discharge-charge measurements at a current rate of 0.1 C as depicted in **Fig. 2a**. The first discharge exhibited two plateaus at 1.70 and 1.10 V, while the first charge process showed two potential plateaus, which are short and prolonged at around 1.85 and 2.25 V, respectively. After the 5th cycle, only one pair of discharge and charge plateaus were observed at 1.73 and 1.85 V, and they are consistent with the reported potential plateaus for Cu_2S [4]. Whereas the discharge plateau at around 1.10 V during the 1st cycle, which is not characteristic for copper sulfides, can be associated with the electrolyte decomposition, thus causing the formation of a passivation film or a solid electrolyte interface (SEI) known to occur on carbon materials [8]. The initial discharge and charge capacities of Cu_2S on CFP are 532 and 379 mAh g^{-1} , respectively. On the following 5th cycle the cell exhibited value of 330 mAh g^{-1} (98% of its theoretical capacity) with approximately 100% Coulombic efficiency.

A CV profile in **Fig. 2b** shows lithiation and delithiation processes at a scan rate of 0.05 mV s^{-1} . The 1st cycle cathodic scan defines two reduction peaks at 1.63 V coming from lithium insertion and at 1.05 V from SEI, respectively. After the 5th cycle, mainly high intensity cathodic peak at about 1.63 V can be observed. Whereas, on the anodic scan at the 1st cycle, two distinct peaks less intense at 1.87 V and sharp at 2.30 V changed after the 5th cycle to the main peak at about 1.87 V and broad at 2.10 V. The results correspond to the charge-discharge voltage profiles in Fig. 2a.

Ex situ XRD analysis of fully discharged and charged electrodes were investigated after disassembling cells to understand actual reaction mechanism of Cu_2S . The XRD peaks after discharge and charge processes of the 1st and 5th cycles are shown in **Figs. 2c** and **2d**. After the first discharge, we can confirm the formation of Cu and Li_2S peaks [18,19], where Li_2S appeared on the overlap with carbon peaks by slightly broadening of CFP peak from its original position at 27 °. The high repetitiveness of peaks can be observed after the completed 5th discharge indicating reversibility of reactions.

As for the charge process in Fig. 2d, after the 1st cycle, we can clearly detect crystal structure change from monoclinic Cu_2S with space group $P2_1/c$ to tetragonal $\text{Cu}_{1.96}\text{S}$ with space group $P4_32_12$ [11]. That might be the reason for the flattening of the 1st oxidation plateau from 2.25 to 1.85 V shown in Fig. 2a. The formed less crystallized $\text{Cu}_{1.96}\text{S}$ during the 1st charge results in the higher voltage plateau at 2.25 V [20]. Furthermore, along with newly formed $\text{Cu}_{1.96}\text{S}$ peaks, we can also detect Cu metal spectra in XRD patterns after the 1st and 5th cycles, and that confirms the oxidation reaction is not reversible to its initial phase of monoclinic Cu_2S . The formed tetragonal $\text{Cu}_{1.96}\text{S}$ peaks appeared with higher intensity on the following 5th cycle, where the plateau flattened to 1.85 V implies that different product with less energy barrier than Cu_2S is formed [20]. The obtained results suggest that the occurred capacity fading during the initial five cycles comes from the irreversibility of the 1st cycle reaction due to the formation of the tetragonal $\text{Cu}_{1.96}\text{S}$ as depicted in XRD patterns. The reaction mechanism of Cu_2S with Li^+ between 1.0 and 3.0 V cut-off range can be expressed for the 1st discharge process, when the lithium ions intercalate between active sites of sulfur and trigger movement of the highly-mobile copper cations, as follows,



and for the following cycles as,



which are reported correspond to the displacement reactions [4,11,18]. The actual reaction mechanism for stoichiometric Cu_2S on CFP defined through reaching near theoretical capacity and consequently efficient consumption of active mass. However, in the fully discharged 5th cycle XRD pattern series of fading $\text{Cu}_{1.96}\text{S}$ reflections were detected, which might relate to a minor amount of unutilized discharge-charge products of Li_2S and $\text{Cu}_{1.96}\text{S}$ during the discharge-charge processes as capacity was around 98 % of its theoretical value.

In order to gradually decrease SEI formation causing irreversible capacity during the 1st cycle and study reaction mechanism at different cut-off voltage windows the cells were cycled between 1.1 and 3.0 V as demonstrated in **Fig. 3a**. The 1st discharge capacity reached 421 mAh g⁻¹ with exhibiting two plateau regions at 1.70 and 1.10 V as in 1.0-3.0 V cut-off range, and the plateau at 1.10 V occurred only at the 1st discharge. While the charge curve had two plateaus at 1.85 and 2.25 V with the capacity of 332 mAh g⁻¹, which decreased after the 5th cycle to 1.85 V with followed gradual increase to 2.1 V and reached 307 mAh g⁻¹. The difference of the 5th charge curve from 1.0-3.0 V might be due to the slower phase transformation from monoclinic Cu_2S to tetragonal $\text{Cu}_{1.96}\text{S}$ than that of at lower discharge cut-off voltage since Li^+ diffusion was lowered by reduced depth of discharge. The consistent profile of CV measurements is displayed in **Fig. 3b**.

Ex situ XRD analysis of fully discharged and charged electrodes in **Figs. 3c** and **3d** after the 1st and 5th cycles at 1.1-3.0 V did not show a significant difference from the 1.0-3.0 V cut-off range. The formation of Cu and Li₂S after discharge was demonstrated after the 1st and 5th cycles in Fig. 3b. After the 5th charge in Fig. 3d it can be seen that the intensity of Cu_{1.96}S peaks is much sharper than in the 1st cycle. This might result in the 1st charge potential plateau flattening from 2.25 V to 1.85 and 2.1 V as well as larger capacity fading compared with that of at 1.0-3.0 V.

Charge-discharge profile of stoichiometric Cu₂S at further increased discharge cut-off voltage of 1.2-3.0 V is shown in **Fig. 4a**. Only one pair of the plateaus is shown after the 1st and 5th cycles for discharge at 1.70 V and charge at 2.25 V, which is flattened after the 5th cycle to 1.85 V similar to other cut-off voltage ranges. Through increasing the discharge cut-off voltage to 1.2 V the formation of SEI plateau at 1.10 V disappeared and the 1st discharge capacity exhibited a value of 338 mAh g⁻¹. After the 5th cycle, we can see the deterioration of the discharge capacity to 280 mAh g⁻¹.

The demonstrated CV results in **Fig. 4b** revealed similar cathodic and anodic scan peaks as in the charge-discharge potential profiles in Fig. 4a. The intensities of the reduction and oxidation peaks were higher after the 5th cycle at 1.2-3.0 V than those of at 1.0-3.0 V and 1.1-3.0 V in Figs. 2b and 3b. Furthermore, we can detect a small shift of the cathodic peak from 1.63 V at the 1st cycle to 1.65 V after the 5th cycle. The observed differences from the lower discharge cut-off voltages could be linked to the slight changes in the reaction products during discharge and charge processes.

XRD patterns of electrodes after the 1st and 5th discharge-charge are shown in **Figs. 4c** and **4d**. After the 1st discharge, we can observe the formation of Cu and Li₂S

peaks along with small but clear $\text{Cu}_{1.96}\text{S}$ peaks at 31.3, 32.6 and 39.1 ° in Fig. 4c. Particularly, after the 5th cycle $\text{Cu}_{1.96}\text{S}$ peaks are sharpening, while Li_2S peak at 27.0 ° is shifted to 27.2 ° closer to the another $\text{Cu}_{1.96}\text{S}$ peak. That might relate to the insertion of Li^+ into Cu_2S structure and followed formation of $\text{Li}_{2-x}\text{Cu}_x\text{S}$ [11,21,22]. The increasing discharge cut-off voltage to 1.2 V did not drive enough Li^+ ions and electrons to trigger movement of Cu from Cu_2S structure to form separated Cu and Li_2S . The increase of intensity of $\text{Cu}_{1.96}\text{S}$ peaks after the 5th discharge indicates that at the cut-off voltage of 1.2-3.0 V the electrode's active mass gradually decrease its utilization.

On the 1st charge process, the phase transformation to tetragonal $\text{Cu}_{1.96}\text{S}$ also was observed, but the difference from the lower cut-off voltage ranges (1.0, 1.1-3.0 V) is that faded Li_2S and some Cu_2S ($\text{Li}_{2-x}\text{Cu}_x\text{S}$) peaks can be additionally detected at 1.2-3.0 V voltage window. This might suggest that after the 1st charge phase transformation to tetragonal $\text{Cu}_{1.96}\text{S}$ happened slower than at 1.0-3.0 V and 1.1-3.0 V. Therefore, the 1st discharge and charge capacities were about theoretical capacity of Cu_2S , which drastically dropped to 280 mAh g⁻¹ after the 5th cycle. Consequently, after the 5th charge all peaks are matching with tetragonal $\text{Cu}_{1.96}\text{S}$. The capacity fading during the initial five cycles might relate to the intensity of the formed products of $\text{Cu}_{1.96}\text{S}$ after charge. The capacity fading was experienced to be less at 1.0-3.0 V in contrast with 1.1-3.0 and 1.2-3.0 V, where the intensity of formed $\text{Cu}_{1.96}\text{S}$ after the 1st and 5th cycles were higher and sharper as revealed in Figs. 3d and 4d.

The cyclability of the cell at different cut-off voltage windows demonstrated in **Fig. 5a** for 50 cycles at 0.1 C rate. Cu_2S coated on CFP exhibited high initial discharge capacity of 532 mAh g⁻¹, which dropped to 330 mAh g⁻¹ (98% of its theoretical capacity) after the third cycle and maintained stable for 20 cycles around

this value with about 100 % Coulombic efficiency between 1.0 and 3.0 V. Further, at the end of the 50th cycle, capacity slightly decreased to 311 mAh g⁻¹. On the other hand, with higher discharge cut-off voltages cells exhibited less charge/discharge capacities. At cut-off voltage range of 1.1-3.0 V discharge capacity was 307 mAh g⁻¹ and at 1.2-3.0 V 280 mAh g⁻¹ after the 5th cycle. To the end of the 50th cycle, cells showed 284 and 266 mAh g⁻¹ for 1.1-3.0 and 1.2-3.0 V, respectively. Coulombic efficiency decreased as well from 100 % at 1.0-3.0 V to 98 % at 1.2-3.0 V, which could be related to the increased internal resistance, since with the increase of discharge voltage energy efficiency delivered by the cells decreased as well. Moreover, due to the phase change from monoclinic Cu₂S to tetragonal Cu_{1.96}S the discharge capacity stabilized only after the third cycle for cut-off range 1.0-3.0 V, while it took 5 cycles for 1.1-3.0 V and 1.2-3.0 V. This tendency is consistent with the *ex situ* XRD results suggesting the slower phase change at higher discharge cut-off voltages.

The slight difference in the discharge capacities can be highlighted when cells were cycled at 1.1-3.0 V and 1.2-3.0 V in Fig. 5a, which might imply that irreversible capacities from SEI formed during the 1st discharge did not significantly affect the electrochemical performance of stoichiometric Cu₂S. From the results, we observed that CFP facilitates Li ions transfer into the electrode, which significantly enhanced utilization of the electrode's active mass and near the theoretical capacity has been exhibited at 1.0-3.0 V cut-off voltage without significant capacity deterioration for 50 cycles. Stoichiometric Cu₂S coated on CFP showed superior results than that of on Al and Cu foils [11] as corrosion of current collector was omitted and exhibited capacities were higher than most of the previously reported results on Cu₂S [4,6-9,20].

To evaluate further electrode stability, we cycled cells at various current rates and **Fig. 5b** shows the cycling performance of Cu₂S on CFP at 1 C for 100 cycles. The

cell at 1.0-3.0 V delivered an initial discharge capacity of 415 mAh g⁻¹ and after the 3rd cycle capacity decreased to 280 mAh g⁻¹ and retained approximately at this value for 100 cycles with 100 % Coulombic efficiency. The discharge capacity of the cell decreased slightly with increasing discharge cut-off voltage. When the cut-off voltages were set at 1.1-3.0 and 1.2-3.0 V the discharge capacities reached an approximately similar value of 250 mAh g⁻¹ and slightly increased after the 20th cycle to 260 mAh g⁻¹ in the case of 1.2-3.0 V. This might happen due to the increased utilization of active material over a long cycling time [11]. To confirm it we carried out *ex situ* XRD analysis of cycled electrodes after the 1st and 50th discharge at 1 C as shown in **Figs. 5c** and **5d**. After the 50th discharge, Cu_{1.96}S peaks formed along with Cu and Li₂S almost disappeared at the cut-off voltage of 1.2-3.0 V compared with that of at the 1st discharge. The discharge reaction became close to the completed reaction of Cu_{1.96}S with Li. While small Cu_{1.96}S peaks had similar intensity after the 1st and 50th discharge at 1.0-3.0 and 1.1-3.0 V, which is consistent with the cycling stability of the cells.

Capacity retention of cells cycled at 1 C rate for 100 cycles was compared in **Fig. 6**. As demonstrated stoichiometric Cu₂S showed excellent capacity retention at various cut-off voltage ranges with the highest value exhibited when it was cycled between 1.0-3.0 V, approximately 90 %. The obvious decrease observed when Cu₂S was cycled between 1.1-3.0 and 1.2-3.0 V to about 83 and 80 %, respectively.

The cycling behavior at different charge-discharge rates between 0.1 and 5 C presented in **Fig. 7**. The 5-cycle performances at higher C-rates are shown in **Fig. 7a** and discharge capacity without severe decline can be observed during cycling at various cut-off voltages. The overall discharge capacity between 0.1 and 5 C was approximately around 300 mAh g⁻¹ demonstrating excellent high rate capability of

stoichiometric Cu_2S coated on CFP at 1.0-3.0 V. The cells at higher discharge cut-off voltages also showed stable capacity retention with very similar discharge capacities for both in overall around 250 mAh g^{-1} , when cycled between 1.1-3.0 V and 1.2-3.0 V.

The first oxidation/reduction curves at different current rates have similar flat one-plateau regions except for the 1st cycle in **Figs. 7(b-d)**. While the initial specific capacity at 0.3 C was 322 mAh g^{-1} and at 5 C it still showed the high reversible capacity of 290 mAh g^{-1} at 1.0-3.0 V cut-off range. The increase of discharge cut-off voltage cannot benefit for the diffusion ability of Li^+ , since the voltage difference between discharge and charge is increased. Therefore, charge-discharge capacities significantly reduced at higher C-rates from 248 mAh g^{-1} at 0.3 C to 213 mAh g^{-1} at 5 C between 1.1-3.0 V. Also from 244 mAh g^{-1} at 0.3 C to 217 mAh g^{-1} at 5 C between 1.2-3.0 V. Additionally, the charge and discharge plateau voltage difference was mostly negligible with only slight increase from approximately 0.13 V at 1.0-3.0 V to 0.15 V at 1.1-3.0 and 1.2-3.0 V. The flat and prolonged plateaus at 1.70 V for discharge and 1.85 V for charge was kept unchanged at different C-rates for cells tested at different cut-off voltages, which implies that the process has good kinetics even at high current rates.

Toward a further understanding of the influences of discharge cut-off voltages on electrochemical performance, electrochemical impedance spectroscopy (EIS) measurements were performed on the cells (1.0~1.2 and 3.0 V) before cycling and after five discharge-charge cycling tests at 0.1 C as shown in **Figs. 8a** and **8b**. The four Nyquist curves are all composed of semicircles in the high-to-medium region and inclined line at the low frequency region. The semicircles are known to be related to the charge transfer resistance (R_{ct}), which comes from the difficulty of charge transfer

between cathode and electrolyte interface, while slope line corresponds to Warburg impedance (R_w) over Li^+ diffusion in the solid materials. The R_{ct} values after the 5th discharge are demonstrated in **Table 1**, where different discharge capacity values were also presented after the 1st, 20th and 50th cycles at various cut-off voltage windows. The EIS results confirmed that the smallest interface barrier occurred at a cut-off voltage of 1.0-3.0 V after the 5th discharge as R_{ct} reached the lowest value compared with those of other cells (1.1, 1.2-3.0 V). The higher R_{ct} resistance was consistent with the higher capacity drop after the 50th cycle. The Nyquist plots were also measured after the 5th charge process as shown in Fig. 8b. We can observe that the charge transfer resistance reduced due to the faster kinetics products of the process during charge ($\text{Cu}_{1.96}\text{S}$) in comparison with discharge (Li_2S). The data difference of R_{ct} at discharge and charge clearly shown in **Fig. 8c**, where charge process R_{ct} is lower at 1.0-3.0, 1.1-3.0 V and gradually increased at 1.2-3.0 V due to the reduced electron transfer. Moreover, Li^+ diffusion could be observed from the R_w slope line, where it was steep at 1.0-3.0 V than those of at 1.1-3.0 V and 1.2-3.0 V, which is in agreement with obtained high capacity results during the high C-rate testing in the case of 1.0-3.0 V cut-off voltage.

4. Conclusions

Successfully synthesized stoichiometric Cu_2S with monoclinic crystal structure coated on CFP exhibited high capacity, excellent cycling stability, and good rate capability. The minor capacity drop and plateau flattening from 2.25 to 1.85 V during the initial cycles could be linked to the phase change from monoclinic Cu_2S to tetragonal $\text{Cu}_{1.96}\text{S}$, which was detected by *ex situ* XRD analysis. Effective electron

path and corrosion prevention on CFP enhanced active material utilization, and near theoretical capacity of Cu_2S 330 mAh g^{-1} was stable for 50 cycles at 0.1 C and 1.0-3.0 V cut-off voltage window. When the cut-off voltage was increased to 1.2-3.0 V to avoid SEI formation and irreversible discharge capacity at the 1st cycle, the cell still exhibited relatively high capacity of 280 mAh g^{-1} at 0.1 C and 250 mAh g^{-1} at 1 C. *Ex situ* XRD analysis showed that the phase transformation during charge, from monoclinic Cu_2S to tetragonal $\text{Cu}_{1.96}\text{S}$, progresses slower at 1.2-3.0 V than that of at 1.0-3.0 V. The reason could come from the incomplete electrochemical reactions, which caused higher charge transfer resistance and lowered kinetics. At higher current rates, stoichiometric Cu_2S on CFP showed excellent capacity retention without severe decay between 0.1 and 5 C at various cut-off voltage windows.

Acknowledgements

This research was partially supported by the Ministry of Education, Culture, Sports, Science and Technology of Japan (Grant No. 15H04251). The authors are also grateful to Mr. J. Koki of the Center for Advanced Materials Analysis (Tokyo Institute of Technology, Japan), for the FE-SEM observation of the material.

References

- [1] H. Li, Z. Wang, L. Chen, X. Huang, Research on Advanced Materials for Li-ion Batteries, *Adv. Mater.* 21 (2009) 4593-4607.
- [2] B. Scrosati, Recent advances in lithium ion battery materials, *Electrochim. Acta* 45 (2000) 2461-2466.
- [3] N. Nitta, F. Wu, J. T. Lee, G. Yushin, Li-ion battery materials: present and future, *Mater. Today* 18 (2015) 252-264.

- [4] B. Jache, B. Mogwitz, F. Klein, P. Adelhelm, Copper sulfides for rechargeable lithium batteries: Linking cycling stability to electrolyte composition, *J. Power Sources* 247 (2014) 703-711.
- [5] C. Shi, X. Li, X. He, J. Zhao, New insight into the interaction between Carbonate-based Electrolyte and Cuprous Sulfide Electrode Material for Lithium Ion Batteries, *Electrochim. Acta* 174 (2015) 1079-1087.
- [6] X. Wang, Y. Wang, X. Li, B. Liu, J. Zhao, A facile synthesis of copper sulfides composite with lithium-storage properties, *J. Power Sources* 281 (2015) 185-191.
- [7] S. Ni, X. Lv, T. Li, X. Yang, Fabrication of Cu_2S cathode for Li-ion battery via a low dry thermal sulfuration method, *Mater. Chem. Phys.* 143 (2013) 349-354.
- [8] X. Meng, S. C. Riha, J. A. Libera, Q. Wu, H. H. Wang, A. B. F. Martinson, J. W. Elam, Tunable core-shell single-walled carbon nanotube- Cu_2S networked nanocomposites as high-performance cathodes for lithium-ion batteries, *J. Power Sources* 280 (2015) 621-629.
- [9] C. -H. Lai, K. -W. Huang, J. -H. Cheng, C. -Y. Lee, B. -J. Hwang, L. -J. Chen, Direct growth of high-rate capability and high capacity copper sulfide nanowire array cathodes for lithium-ion batteries, *J. Mater. Chem.* 20 (2010) 6638-6645.
- [10] W.-Y. Kim, B. M. Palve, H. M. Pathan, O.-S. Joo, Spray pyrolytic deposition of polycrystalline Cu_2S thin films, *Mater. Chem. Phys.* 131 (2011) 525-528.
- [11] G. Kalimuldina, I. Taniguchi, Synthesis and electrochemical characterization of stoichiometric Cu_2S as cathode material with high rate capability for rechargeable lithium batteries, *J. Power Sources* 331 (2016) 258-266.
- [12] M. Konarova, I. Taniguchi, Synthesis of carbon-coated LiFePO_4 nanoparticles with high rate performance in lithium secondary batteries, *J. Power Sources* 195 (2010) 3661-3667.

- [13] S. -H. Chung, A. Manthiram, Low-cost, porous carbon current collector with high sulfur loading for lithium-sulfur batteries, *Electrochem. Comm.* 38 (2014) 91-95.
- [14] Y. Liu, B. Jin, Y. F. Zhu, X. Z. Ma, X. Y. Lang, Synthesis of Cu₂S/carbon composite with improved lithium storage performance, *Int. J. Hydrogen Energy* 40 (2015) 670-674.
- [15] L. Yang, S. Cheng, Y. Ding, X. Zhu, Z. L. Wang, M. Liu, Hierarchical Network Architectures of Carbon Fiber Paper Supported Cobalt Oxide Nanonet for High-Capacity Pseudocapacitors, *Nano Lett.* 12 (2012) 321-325.
- [16] I. Taniguchi, C. K. Lim, D. Song, M. Wakihara, Particle morphology and electrochemical performances of spinel LiMn₂O₄ powders synthesized using ultrasonic spray pyrolysis method, *Solid State Ionics* 146 (2002) 239-247.
- [17] R. W. Potter II, H. T. Evans Jr., Definitive X-ray powder data for covellite, anilite, djurleite, and chalcocite, *J. Research U.S. Geol. Surv.* 4 (1976) 205-212.
- [18] A. Debart, L. Dupont, R. Patrice, J. -M. Tarascon, Reactivity of transition metal (Co, Ni, Cu) sulphides versus lithium: The intriguing case of copper sulphide, *Solid State Sci.* 8 (2006) 640-651.
- [19] J. -S. Chung, H. -J. Sohn, Electrochemical behaviors of CuS as a cathode material for lithium secondary batteries, *J. Power Sources* 108 (2002) 226-231.
- [20] Y. Fu, A. Manthiram, Electrochemical properties of Cu₂S with ether-based electrolyte in Li-ion batteries, *Electrochim. Acta* 109 (2013) 716-719.
- [21] N. Yamakawa, M. Jiang, C. P. Grey, Investigation of the Conversion Reaction Mechanisms for Binary Copper (II) Compounds by Solid-State NMR Spectroscopy and X-ray Diffraction, *Chem. Mater.* 21 (2009) 3162-3176.

[22] A. Beleanu, Ternary Lithium Based Compounds Used for Technological Applications, Pharmazie und Geowissenschaften der Johannes Gutenberg-Universität Mainz, 2014. Doctoral dissertation.

Table 1 Discharge capacity and charge transfer resistance of stoichiometric Cu_2S electrode on CFP at 0.1 C rate and various cut-off voltages.

Cut-off range / V	1 st cycle / mAh g ⁻¹	20 th cycle / mAh g ⁻¹	50 th cycle / mAh g ⁻¹	R_{ct} / ohm
1.0-3.0	532	321	311	8.84
1.1-3.0	421	298	284	11.69
1.2-3.0	338	285	266	12.01

Figure captions

Fig. 1. XRD spectra of stoichiometric Cu₂S. Inset: SEM image of powders.

Fig. 2. (a) Charge-discharge voltage profiles vs. capacity of stoichiometric Cu₂S coated on a CFP at a cut-off voltage of 1.0-3.0 V at 0.1 C; (b) Cyclic voltammetry at a scan rate of 0.05 mV s⁻¹ between 1.0-3.0 V; (c) XRD patterns of the fully discharged electrode at the 1st and 5th cycles; (d) XRD patterns of the fully charged electrode at the 1st and 5th cycles.

Fig. 3. (a) Charge-discharge voltage profiles vs. capacity of stoichiometric Cu₂S coated on a CFP at a cut-off voltage of 1.1-3.0 V at 0.1 C; (b) Cyclic voltammetry at a scan rate of 0.05 mV s⁻¹ between 1.1-3.0 V; (c) XRD patterns of the fully discharged electrode at the 1st and 5th cycles; (d) XRD patterns of the fully charged electrode at the 1st and 5th cycles.

Fig. 4. (a) Charge-discharge voltage profiles vs. capacity of stoichiometric Cu₂S coated on a CFP at a cut-off voltage of 1.2-3.0 V at 0.1 C; (b) Cyclic voltammetry at a scan rate of 0.05 mV s⁻¹ between 1.2-3.0 V; (c) XRD patterns of the fully discharged

electrode at the 1st and 5th cycles; (d) XRD patterns of the fully charged electrode at the 1st and 5th cycles.

Fig. 5. Cycle performance of stoichiometric Cu₂S coated on a CFP at various cut-off voltage ranges between 1.0, 1.1, 1.2 and 3.0 V: (a) at 0.1 C for 50 cycles and (b) at 1 C for 100 cycles with Coulombic efficiencies; (c) XRD after the 1st discharge at 1 C; (d) XRD after the 50th discharge at 1 C.

Fig. 6. Capacity retention of stoichiometric Cu₂S at various cut-off voltage windows at 1 C rate for 100 cycles.

Fig. 7. (a) Rate performance of stoichiometric Cu₂S from 0.1 to 5 C at various cut-off voltage ranges; Charge-discharge voltage profiles vs. capacity between: (b) 1.0-3.0 V; (c) 1.1-3.0 V; (d) 1.2-3.0 V.

Fig. 8. Electrochemical impedance spectra (EIS) of stoichiometric Cu₂S coated on a CFP (a) after the 5th discharge, (b) after the 5th charge and (c) relationship between charge-transfer resistance R_{ct} and lower cut-off voltage.

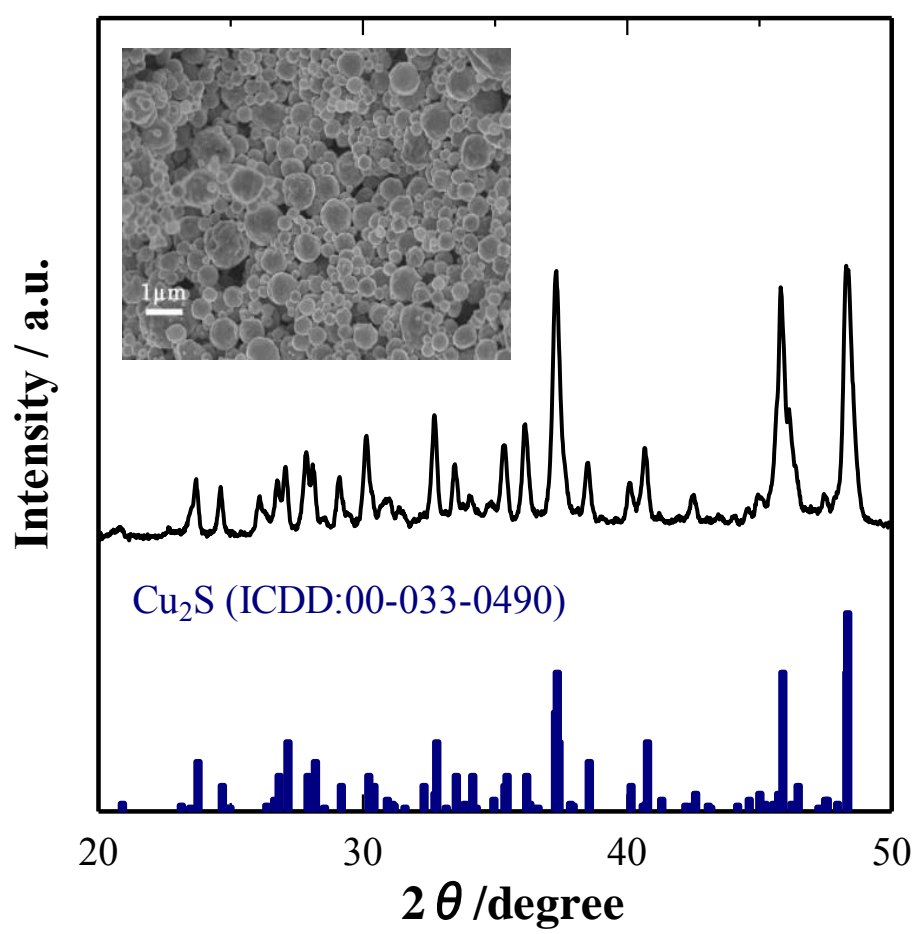
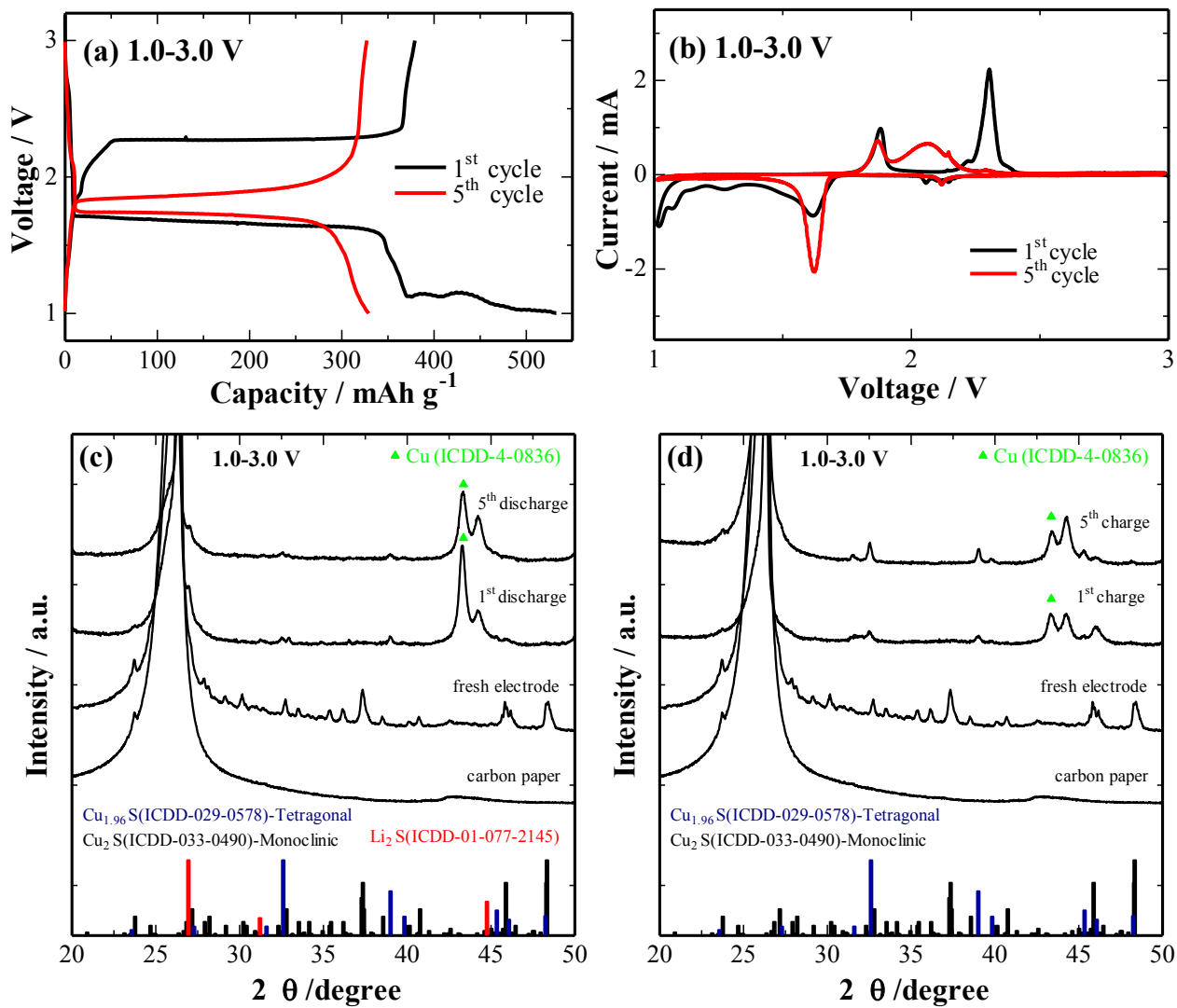


Fig.1

**Fig.2**

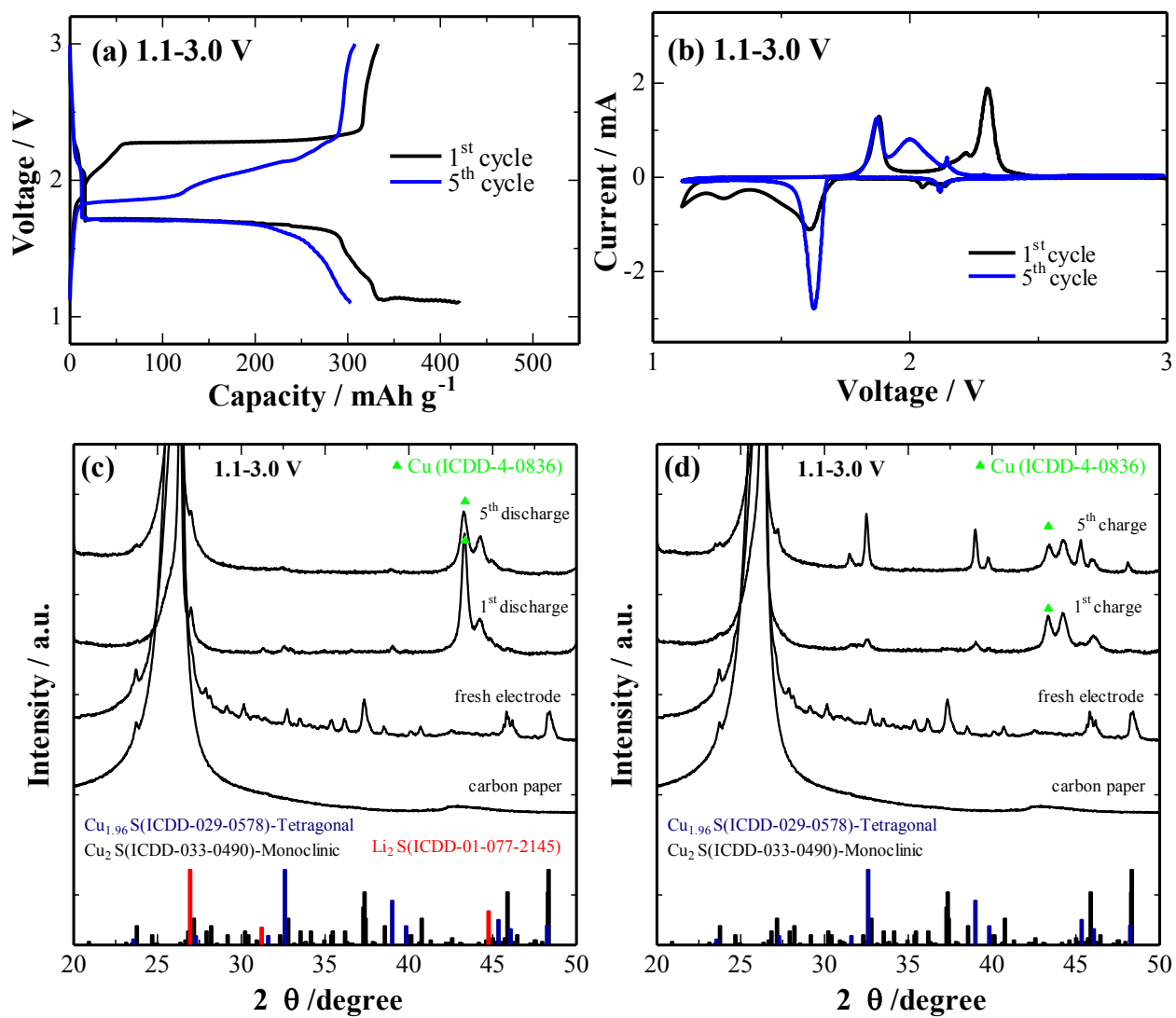
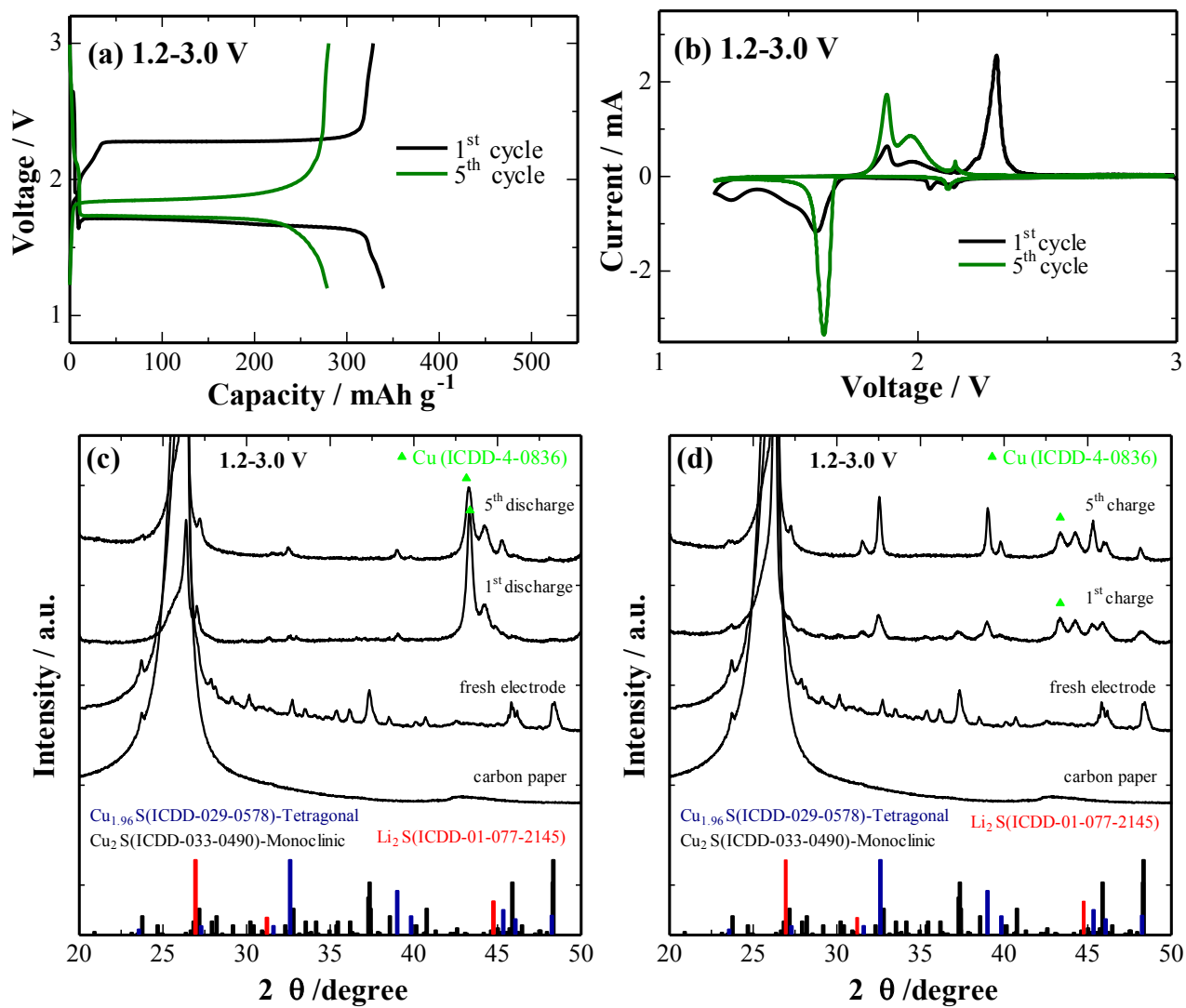


Fig.3

**Fig.4**

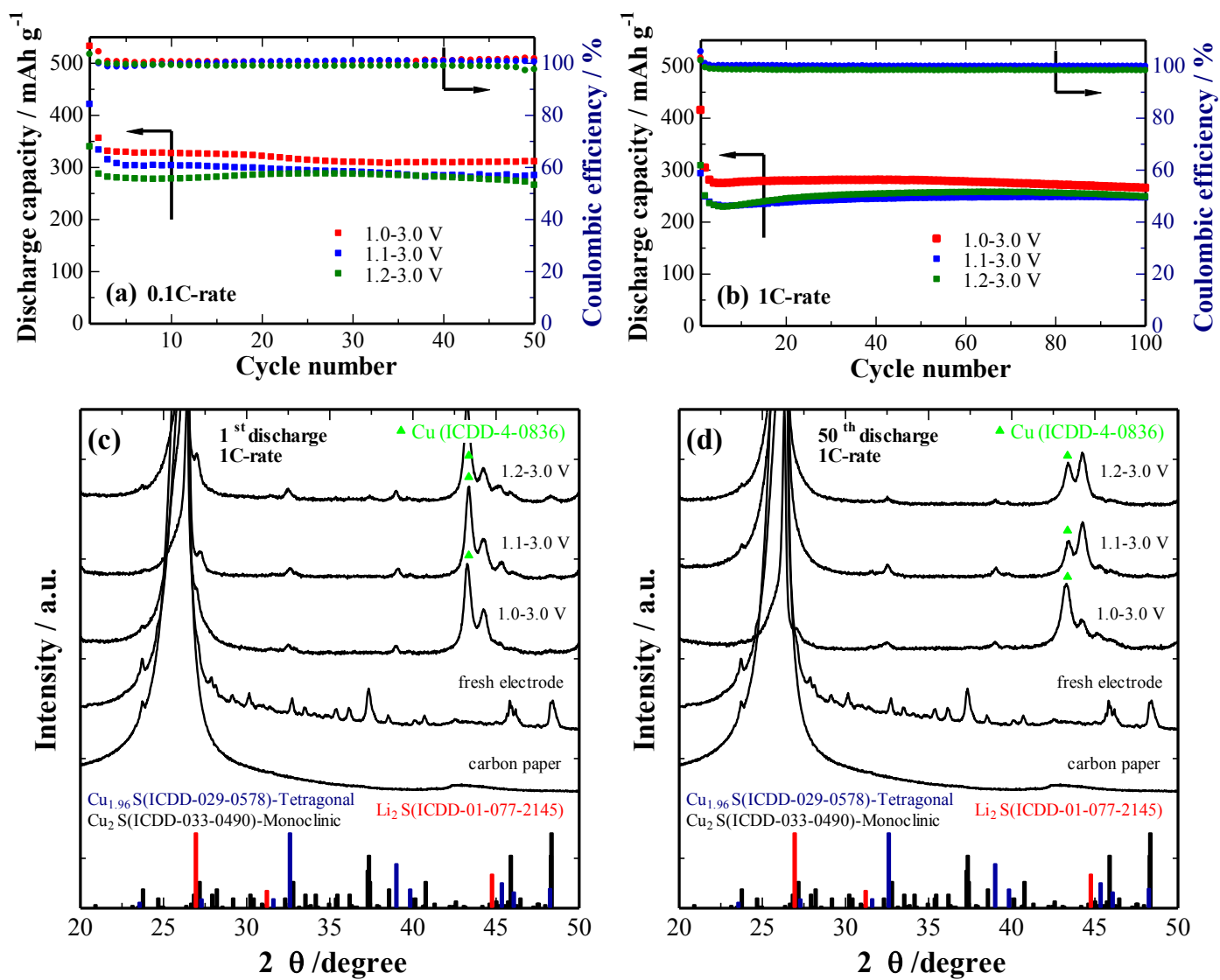


Fig.5

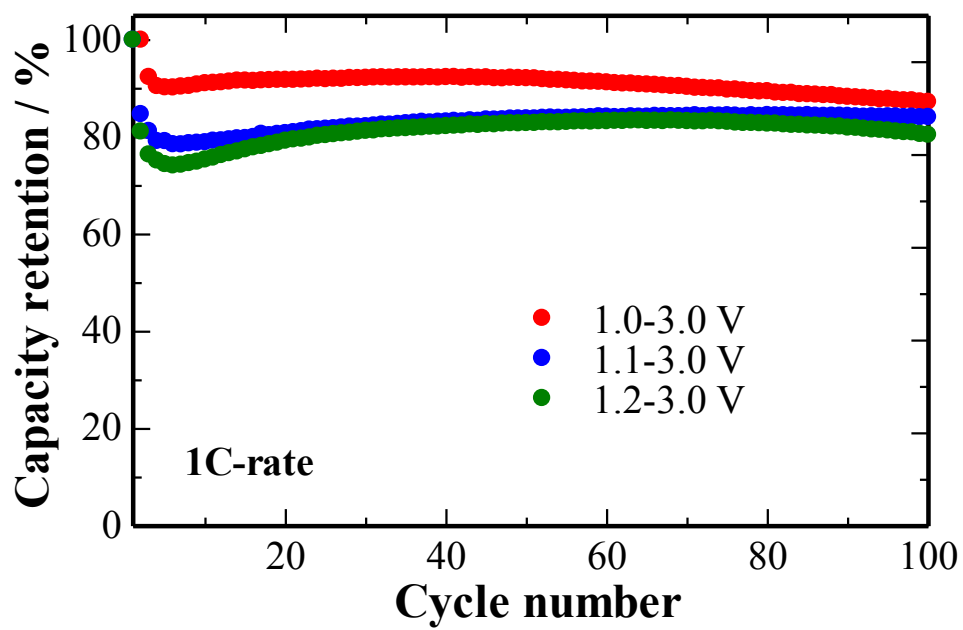


Fig.6

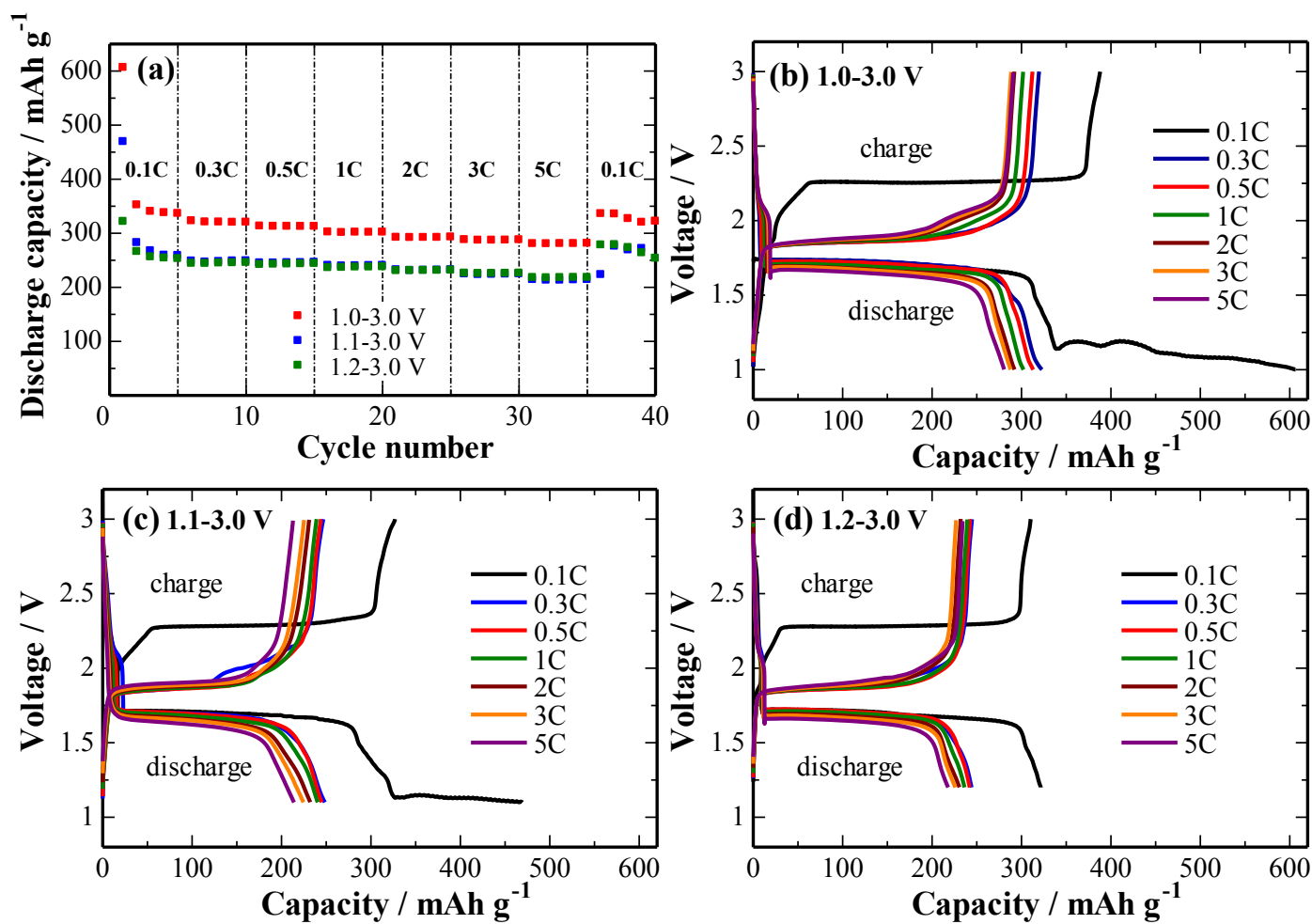


Fig. 7

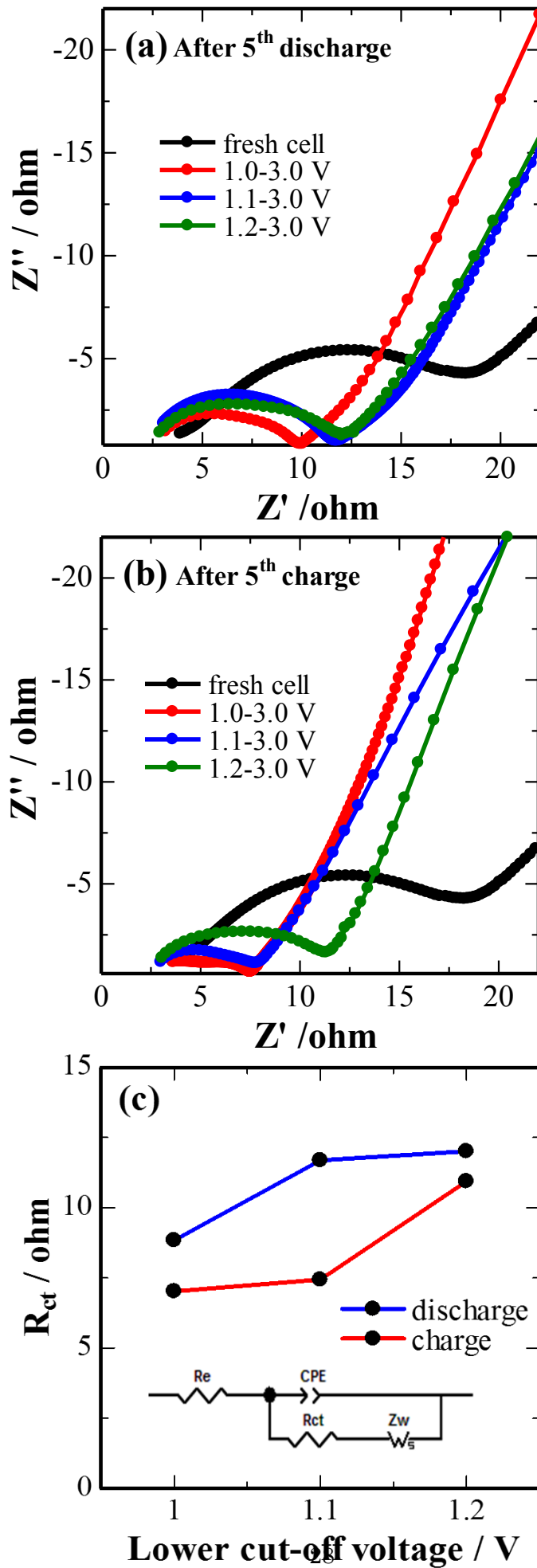


Fig.8